CHAPTER 238

Development of a Numerical Simulation Method for Predicting the Settling Behavior and Deposition Configuration of Soil Dumped into Waters

Kazuki Oda[1] and Takaaki Shigematsu [1]

Abstract

A numerical simulation method, which combines the Marker And Cell method and the Discrete Element Method, for analyzing the settling behavior and deposition configuration of the particles dumped into waters is described. Some calculated results are compared with the experimental ones, and what the settling behavior of the particles and the deposition configuration on the water bottom depend on is discussed.

1. Introduction

In recent years in Japan, large–scale man–made islands such as offshore ports and airports in coastal areas have been increasing in number. They are constructed in general by reclamation with a large volume of soil dumped from a split–hull barge. Hence, from the view point of both the construction management and environmental conservation, it has become very important to predict accurately the settling behavior and deposition configuration of soil. While there are a few studies (Oda, 1989 ; Matsumi, 1992) which treated these problems, their studies can not predict them accurately because in which the interaction of an ambient fluid motion and a particle motion is not taken into consideration in theoretical analyses.

In the present study, a new numerical simulation method for predicting more accurately the settling behavior and deposition configuration of soil particles

[1]Dept. of Civil Engrg. Osaka City Univ. 3-3-138, Sugimoto, Sumiyoshi-ku, Osaka, 558

dumped into waters is developed, and what the settling behavior and deposition configuration depend on is discussed.

2. Simulation Method

The developed numerical simulation method consists of two phases; one is for analyzing the motion of each particle and the other is for analyzing the ambient fluid motion. In this paper the two dimensional calculation procedure will be presented(Oda, 1991).

2.1 Calculation of Particle Behavior

The motion of each particle is calculated by using the Discrete Element Method (the DEM) (Cundall, 1974) which is considered to be useful in analyzing the dynamic behavior of granular assembly.

The momentum and rotational momentum equations of particle i are written

$$(m_i + m_i')\dot{u}_{pi} = \sum_j [F_x]_{ij} + f_x \tag{1}$$

$$(m_i + m_i')\dot{w}_{pi} = \sum_j [F_z]_{ij} + f_z \tag{2}$$

$$(I_i + I_i')\dot{\omega}_{pi} = \sum_j [M]_{ij} \tag{3}$$

where m_i and m_i' are the mass and added mass of particle i respectively, I_i and I_i' are the inertia and added inertia moment, u_{pi}, w_{pi} are the horizontal and vertical velocity component of the particle, ω_{pi} is the rotational angular velocity of the particle, $[F_x]_{ij}$ and $[F_z]_{ij}$ are the horizontal and vertical component of the force exerted between the particles i and j by their contact, $[M]_{ij}$ is the rotational moment resulted from the contact with the particles i and j, f_x and f_z are the fluid forces, "$\cdot$" represents the derivative by time, and $\sum_j$ represents the sum with respect to every particle which contacts with particle i.

The forces $[F_x]_{ij}$, $[F_z]_{ij}$ and moment $[M]_{ij}$ are calculated by

$$[F_x]_{ij} = -[f_n]_{ij} \sin\alpha_{ij} + [f_s]_{ij} \cos\alpha_{ij} \tag{4}$$

$$[F_z]_{ij} = -[f_n]_{ij} \cos\alpha_{ij} - [f_s]_{ij} \sin\alpha_{ij} + V_i \rho_p g \tag{5}$$

$$[M]_{ij} = -\frac{d_i}{2}[f_s]_{ij} \tag{6}$$

where ρ_p is the particle density, V_i is the particle volume, g is the acceleration due to the gravity, d_i is the diameter of particles i, α_{ij} is the angle between x axis and the segment of line which connects the center of particles i and j. $[f_n]$ and $[f_s]$ are the normal and tangential forces caused from their contact between the particles i and j, which are represented

$$[f_n]_{ij} = K_n\delta_n + \eta_n\delta_n/\Delta t_{DEM} \tag{7}$$

$$[f_s]_{ij} = K_s\delta_s + \eta_s\delta_s/\Delta t_{DEM} \tag{8}$$

where K is the spring constant, η is the damping coefficient, δ is the relative displacement between the particles i and j during the time interval Δt_{DEM}, and the subscripts n and s represent the normal and tangential direction.

With the assumption that taking only the drag forces as fluid forces into consideration, the fluid forces acting on the particle i are written

$$f_x = -\frac{1}{2}C_D A_i \rho_f (u_p - u_f)\sqrt{(u_p - u_f)^2 + (w_p - w_f)^2} \tag{9}$$

$$f_z = -\frac{1}{2}C_D A_i \rho_f (w_p - w_f)\sqrt{(u_p - u_f)^2 + (w_p - w_f)^2} - \rho_f g V_i \tag{10}$$

$$C_D = \frac{24}{R_e} + C_{D0}, \qquad C_{D0} = 2.0 \tag{11}$$

$$R_e = \frac{d_i\sqrt{(u_p - u_f)^2 + (w_p - w_f)^2}}{\nu} \tag{12}$$

where ρ_f is the fluid density, A_i is the cross sectional area, ν is the coefficient of kinematic viscosity.

The interaction between particles and fluids is taken into account by calculating the drag force by using the relative particle velocity to the fluid given by Eq.(11).

The each particle acceleration at given time is calculated by solving Eqs.(1)~(3) explicitly, subsequently the velocity and location of each particle are determined.

2.2 Calculation of fluid motion

No calculation method will be presently available to analyze the ambient fluid motion caused by settling of a particle cloud. Edge and Dysart(1972) developed a model with the assumption that dumped material may behave as a dense liquid moving in waters. In the present method, an ambient fluid motion driven by a particle motion is analyzed by means of the MAC method under the assumption that the differences of the density of liquid–solid fluid which contains the particles may cause the motion of fluid.

The equation of continuity and momentum are respectively

$$\frac{\partial u_f}{\partial x} + \frac{\partial w_f}{\partial z} = 0 \tag{13}$$

$$\frac{\partial u_f}{\partial t} + u_f\frac{\partial u_f}{\partial x} + w_f\frac{\partial u_f}{\partial z} = -\frac{1}{\rho_f}\frac{\partial p}{\partial x} + \varepsilon_x\frac{\partial^2 u_f}{\partial x^2} + \varepsilon_z\frac{\partial^2 u_f}{\partial z^2} \tag{14}$$

$$\frac{\partial w_f}{\partial t} + u_f \frac{\partial w_f}{\partial x} + w_f \frac{\partial w_f}{\partial z} = -\frac{1}{\rho_f}\frac{\partial p}{\partial z} + \frac{\rho}{\rho_f} g + \varepsilon_x \frac{\partial^2 w_f}{\partial x^2} + \varepsilon_z \frac{\partial^2 w_f}{\partial z^2} \tag{15}$$

where ρ is the density of liquid–solid fluid which is evaluated as the mean density of liquid and particles, of which locations are determined by the DEM at some given time, in each numerical cell and ε is the coefficient of kinematic eddy viscosity which is calculated as follows

$$\varepsilon = 4 + 0.26 v_0 + 32 \times 10^{-3} v_0^2 \tag{16}$$

where v_0 is the fluid velocity component.This equation comes from the experimental observation by the ocean and meteorological agency in Nagasaki.

3. Calculation Condition

Some vertically two dimensional numerical simulations are performed in order to obtain the settling and dispersion behavior of particles dumped into waters from the water surface. The bottom of a container for dumping of particles is fixed on the water surface. After particles are arranged with short distances between other particles in the container, only the motion of each particle is calculated by using only the DEM until every particle stops to become stable in the condition of keeping the container bottom closed. Then the container bottom is opened, the motion of the particles and fluid are calculated.

According to making reference Kiyama (1983) 10^{-6} sec is used for Δt_{DEM}. The value of the constants in the mathematical models are summarized in Table.1.

The calculation domain is taken between -50cm and +50cm in the horizontal direction for the MAC method and the cell size is taken constant: $\Delta x = 2.5$cm. The movements of particles and ambient flows are analyzed for the different water depths from 10cm to 100cm . The number of interior cells in the vertical direction is constant 40. The time step used in calculation is $\Delta t_{MAC} = 10^{-5}$ sec.

4. Calculated Results

4.1 Comparison with the experimental results

Fig.1 shows the calculated results of the settling and dispersion behavior of the particles with d=0.3 cm diameter, of which the volume is 20 cm^3/cm, and the

Table 1. Values of the Constants in the Mathematical Model

Spring Constant	$K_n/\rho_p g = 4.23 \times 10^4$ (cm) $K_s/\rho_p g = 1.05 \times 10^4$ (cm)
Dumping Coefficient	$\eta_n/\rho_p g = 2.47$ (cm· s) $\eta_s/\rho_p g = 1.24$ (cm· s)
Friction Coefficient	$\tan\mu$=30 °

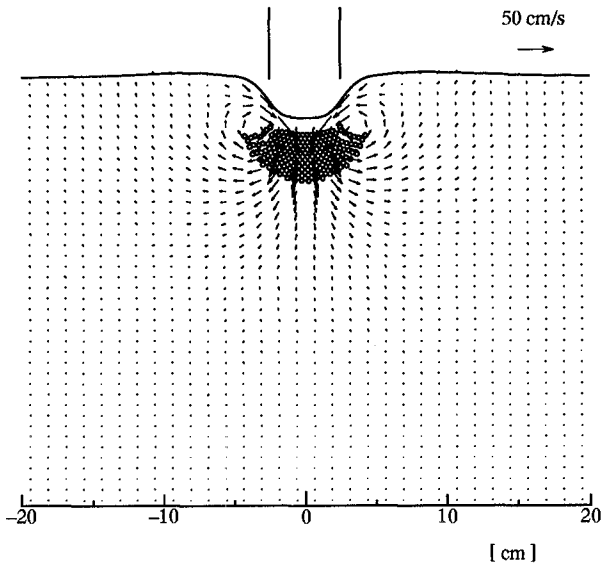

(a) $t = 0.2$ sec

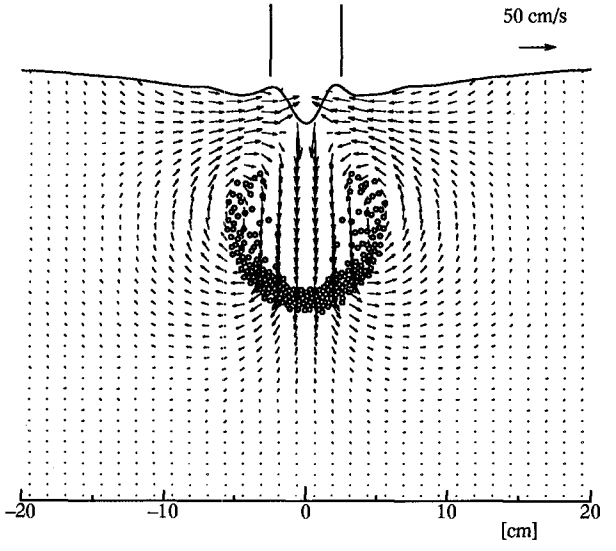

(b) $t = 0.4$ sec

Fig. 1. Calculated results

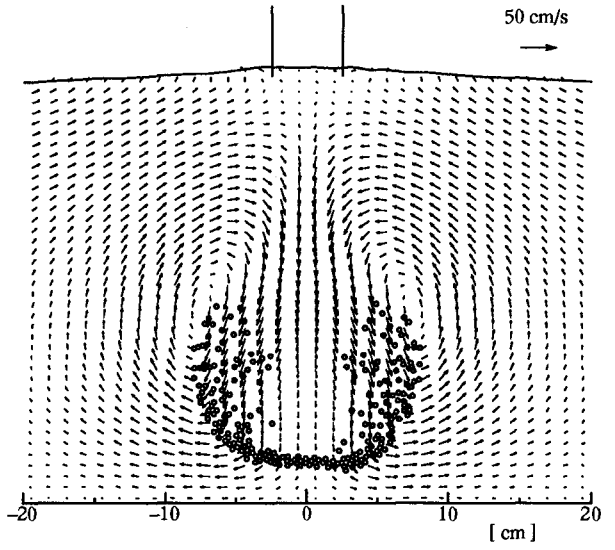

(c) $t = 0.7$ sec

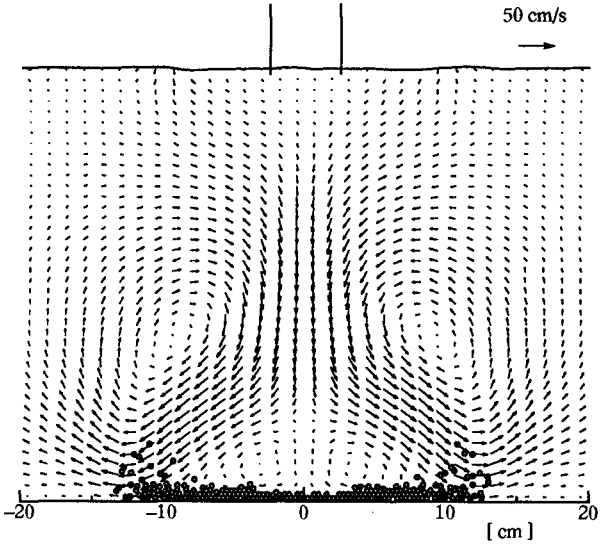

(d) $t = 1.0$ sec

Fig. 1. Calculated results

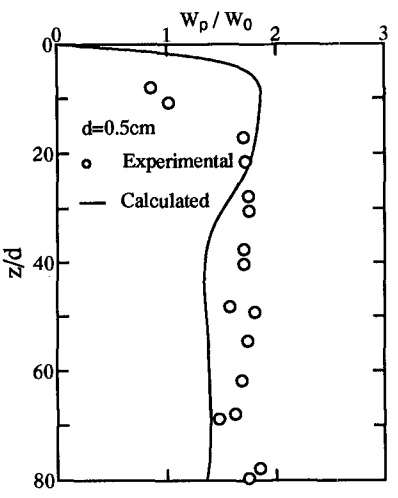

Fig. 2. Settling velocity of a particle cluster

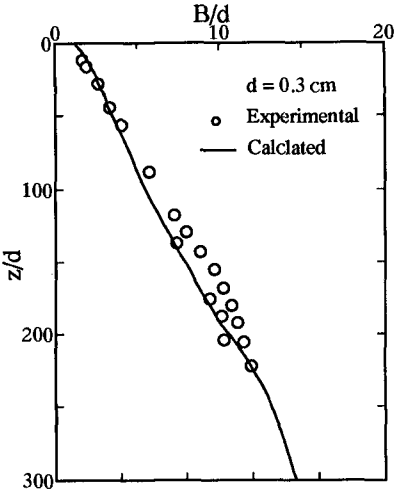

Fig. 3. Dispersion width of a particle cluster

movements of the ambient fluid flow at the specific time after dumping under the condition of water depth h=30 cm and instantaneous opening of the container bottom of which width b_0 is 5cm. From Fig.1, it may be seen that the particles are settling as a cluster rather than individuality. These calculated results show a similar tendency to the experimental ones by Murota et al.(1988).

Fig.2 shows the comparison of the calculated results with the experimental ones on the settling velocity of the particle cluster. The settling velocity W_p is normalized by $W_0 = \sqrt{(\rho_p/\rho_f - 1)gd}$. Similarly the comparison of the calculated results with the experimental ones on the dispersion width B of the cluster in settling is shown in Fig.3. From Figs.2 and 3, it would be said that the present method can predict reasonably well the settling and dispersion behavior of particles.

4.2 Deposition configurations and water depth

The distributions of the relative number of particles passing through per unit width of the horizontal plane at z/h =0.2, 0.4, 0.6, 0.8 and 1.0 in the case of h=10, 30, 50 and 100 cm are shown in Fig.4. It should be noted that the distribution of relative number at z/h=1.0 displays the deposition configuration of particles at rest on the water bottom. It is found in Fig.4(b) that for h=30cm the distribution has two peaks at z/h=0.4 and the distance between two peaks becomes wider as the particles settling deeper. The deposition configuration on the bottom seems to be a mountain with two peaks. It can be seen in Fig.4 (c) that with settling of

particles two peaks are separated farther, those heights become smaller and the final deposition configuration becomes flatter. For h=100cm, the distribution seems to be almost uniform at z/h=0.6 and subsequently the width and the height of the distribution become much wider and lower. These tendencies coincide with Mutoh's experimental results (1974).

Based on the experimental observation, he presumed that an increase in the horizontal fluid velocity near the bottom with the water depth induced an increase in the horizontal velocity of the particles near the bottom. But from the present calculated results it would be considered that the deposition configuration of the particles significantly depends on the dispersion behavior of the particles in the process of settling.

4.3 Settling behavior of particles and opening angular velocity of the container

Fig.5 shows the calculated results of the variation of space positions of particles and fluid velocity field at the moment of the contact of their lowest part with the water bottom with the opening angular velocity of the container bottom for h=30cm. From the calculated result for ω = 30 deg./s, each particle seems to be settling individually with characteristic of a single particle. But the particles for ω=60 deg./s would be settling as a cluster as shown in Fig.5(b). The cluster of the particles for ω=90 deg./s becomes larger than one for ω=60deg./s.

The same calculations for h=10 and 50 cm were performed. Based on those results for h=10cm, we could not see any longer the cluster of particles in settling even in the case of ω=90 deg./s. But for h=50cm the clusters could be seen in every case of ω=30, 60, 90 deg./s and became larger with an increase of the opening angular velocity of the container bottom. It is found, therefore, that the settling behavior of particles gets to depend more and more on the opening angular velocity of the container with in increase of the water depth.

4.4 Deposition configuration and opening angular velocity of the container

The deposition configurations under the condition of the particle volume V_0=20 cm^3/cm, particle diameter d=0.3 cm, the container width b_0=5cm, ω=30, 60, 90 deg./s, and h= 10, 30, 50 cm are calculated. From the calculated results as shown in Fig.6, it is found that the opening angular velocity of the container bottom does not effect on the deposition configurations in the case of h=10 and 30 cm, but that for h=50cm the deposition width and height become wider and lower with an increase of the opening angular velocity. When the particles are dumped into waters with some opening angular velocity of the container bottom,

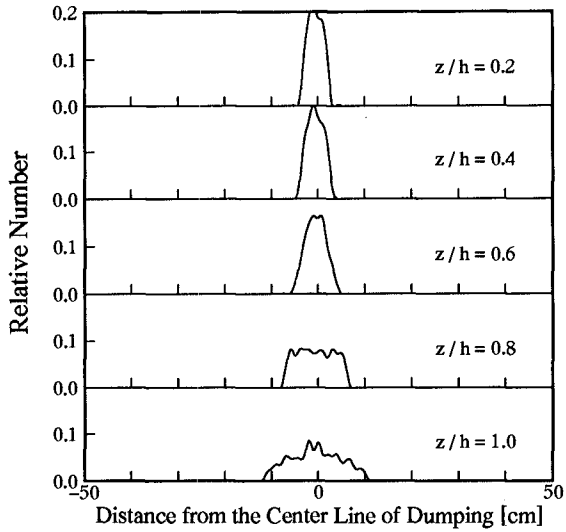

(a) h=10cm

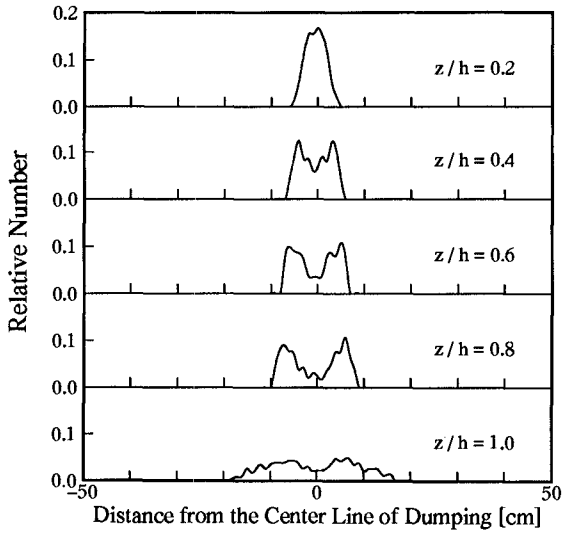

(b) h=30cm

Fig. 4. Distribution of Relative Number of Particles Passing through the Horizontal Plane

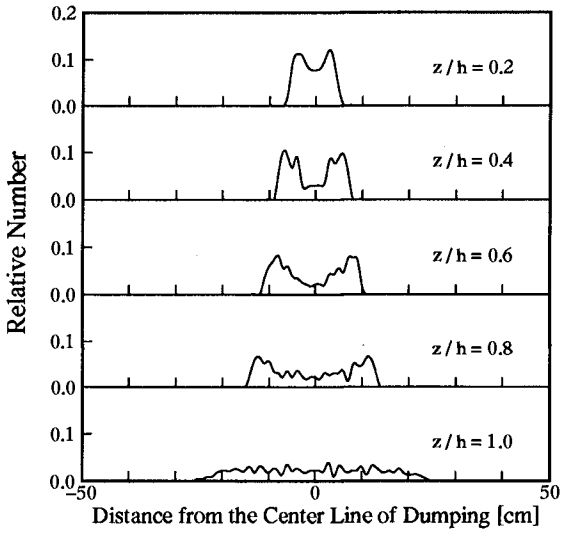

(c) h=50cm

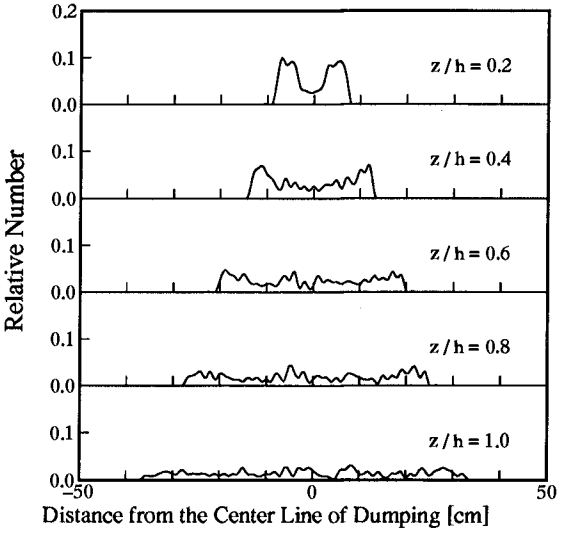

(d) h=100cm

Fig. 4. Distribution of Relative Number of Particles Passing through the Horizontal Plane

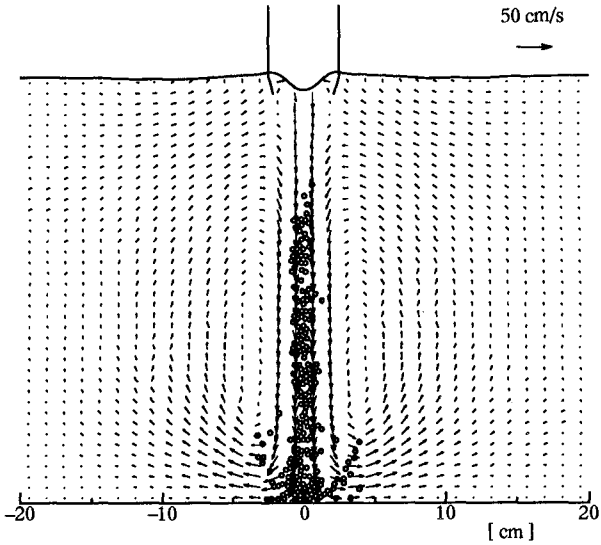

(a) ω=30 deg./s

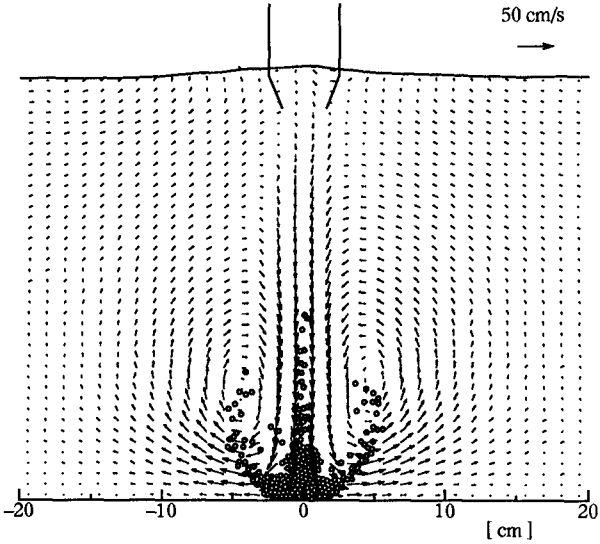

(b) ω=60 deg./s

Fig. 5. Calculated results

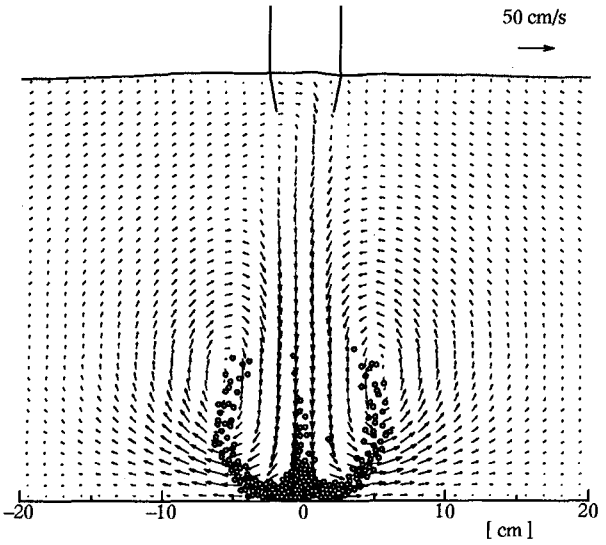

(c) ω= 90 deg./s

Fig. 5. Calculated results

the particles settle as a cluster on condition that the water depth and opening angular velocity are larger and the particle cluster grows larger with an increase of the water depth as described in section 4.3. Hence, it would be thought that the growth of the cluster of particles in settling effects on the deposition configuration.

4.5 Effect of the container width and the volume of dumped particles on dispersion width

The calculated results concerning the effect of the container width on a dispersion configuration when the volume of dumped particles is constant V_0= 20cm^3/cm and the water depth is h=30 cm, are shown in Fig.7. The dispersion widths of particles in settling for b_0=2.5 and 5.0 cm are almost the same and the deposition widths in both cases are also almost the same. But the dispersion and deposition widths for b_0=10 cm are different from those for other cases.

Fig.8 shows the calculated results concerning the effect of the dumped volume V_0 on the dispersion width under the condition that the container width is

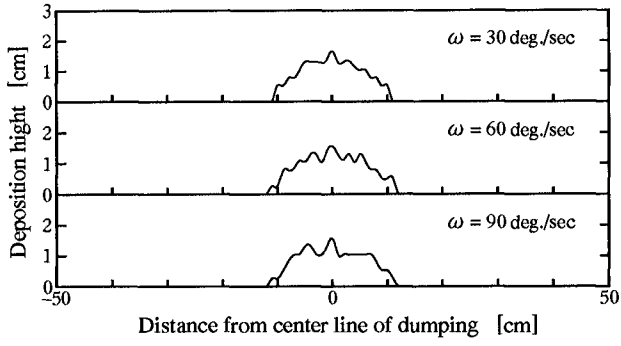

(a) $h = 10$ cm

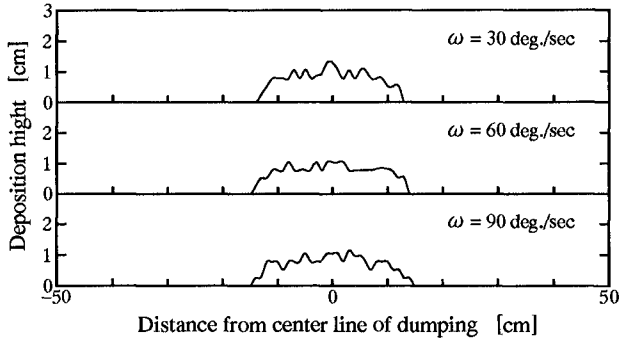

(b) $h = 30$ cm

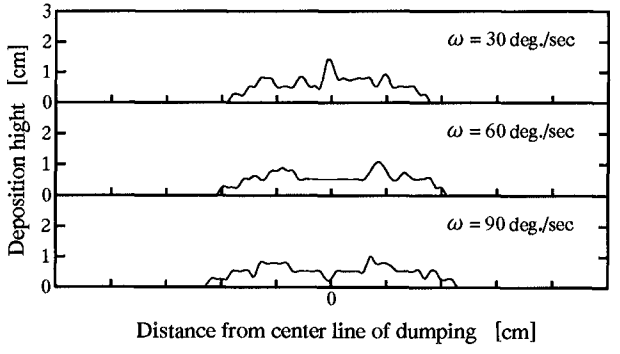

(c) $h = 50$ cm

Fig. 6. Variation of the deposition configuration with the opening angular velocity of container bottom

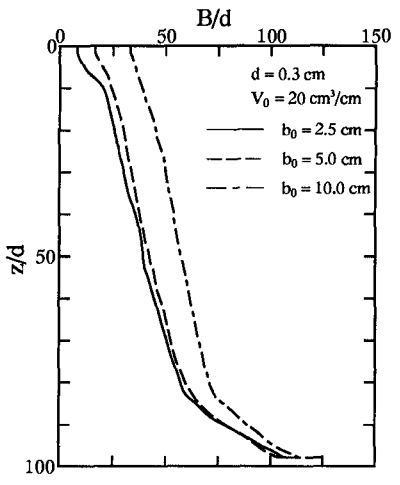

Fig. 7. Variation of dispersion width with container width

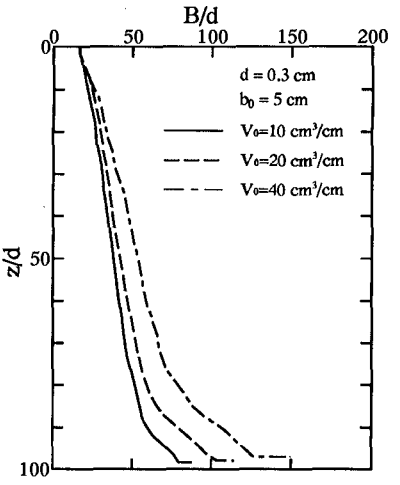

Fig. 8. Variation of dispersion width with the volume of particles

constant b_0=5.0cm and the water depth is h=30 cm. The dispersion width in settling and the deposition width on the water bottom become wider with an increase of the volume of dumped particles. Moreover what is evident comparing Fig.7 with Fig.8 is that the deposition width depends on the volume of dumped particles much more than the container width under the present calculation condition.

5. Conclusions

A calculation method for analyzing simultaneously the settling and dispersion behavior of particles and ambient fluid motion simultaneously was developed. It was founded that the calculated results of those behavior by the present method were reasonably good agreement with the experimental ones. Moreover the deposition configurations were calculated under the condition of the various water depths, container width, volume of dumped particles, and opening angular velocity of the container. The obtained results are summarized as follows :

(1) The dispersion width of the settling particles and deposition width on the water bottom become wider with an increase of the volume of dumped particles.

(2) The deposition width depends on the volume of dumped particles rather than the container width.

(3) The deposition configuration depends on the water depth and it is influenced by the dispersion behavior of settling particles.

(4) The increase of the opening angular velocity makes the deposition width wider in deeper water but it has few effect on the deposition configuration in shallower water.

References

[1] Cundall,P.A. (1974) : Rational Design of Tunnel Supports – A Computer Model for Rock Mass Behavior Using Interactive Graphics for the Input and Output of Geometrical Data, Technical Report MRD-2-74, Missouri River Division, U.S.Army Corps of Engineers.

[2] Edge, B.L. and B.C. Dysart (1972) : "Transport mechanisms governing sludges and other materials barged to sea. " Civil Engineering and Environmental Systems Engineering, Clemson University.

[3] Oda K., T. Higuchi and K. Iwata (1989) : "Studies on Deposition–Mound Configurations of Quarry Stones Discharged from a Split–Hull Barge", Proc. of Coastal Engineering, JSCE Vol.36, pp.814–818, (in Japanese).

[4] Oda K., T. Shigematsu and K. Ujimoto (1991) : "Descent and Dispersion Analysis of Dumped Particles in Waters by Means of a Combined-DEM–MAC method", Loquid–Solid Flows –1991, pp.159–163.

[5] Matsumi Y. and A. Kimura (1992) : "Hydraulic Approach to Determining Optimum Interval of Discharge Sites of Barge in Constructing Rubble Foundation of Deep Water Breakwater", 23rd Inter. Conf. on Coastal Engrg. ASCE, pp.3149–3162.

[6] Kiyama H. and H. Fujiyama (1983) : "Application of Cundall's Discrete Block Method to Gravity Flow Analysis of Rock–like Granular Materials", Proc. of Japan Society of Civil Engineers, No.333, pp.137–146. (in Japanese)

[7] Mutoh A., S. Yoshii and T. Ishida (1974) : "Sand Heap Undulation on the Sea Bed by the Bottom–Dumped Barge for Large Scale Land Reclamation", Mitsubishi Heavy Industry Technical Review, Vol.11, No.1, pp.92–104.

[8] Murota A., K. Nakatsuji, M. Tamai and H. Machida (1988) : "Formation of solid–and–fluid buoyancy cloud in reclining works", Proc. of the 35th Japanese Conference on Coastal Engineering pp.777-781.